11th Australasian Fluid Mechanics Conference
University of Tasmania, Hobart, Australia
14-18 December 1992

A STUDY OF THE INLET VORTEX IN A CENTRIFUGAL FAN

P. CHEN[1], M. SOUNDRA-NAYAGAM[2], A.N. BOLTON[2] and H.C. SIMPSON[1]

[1]Dept Mechanical & Process Engineering, University of Strathclyde, Glasgow, UNITED KINGDOM

[2]Flow Centre, National Engineering Laboratory, East Kilbride, Glasgow G75 0QU, UNITED KINGDOM

ABSTRACT

The unstable behaviour of the inlet vortex has been studied in an industrial centrifugal fan fitted with inlet vanes. The frequency of the pressure fluctuations caused by the vortex was found to increase with flow rate and the inlet swirl angle. At a constant swirl angle, the frequency had a linear variation with the flow rate while the amplitude of the pressure fluctuations increased exponentially with the flow rate. In all cases the maximum pressure fluctuation occurred at the fan inlet. The structure of the inlet vortex was studied using a 5-hole probe and also using a phase locked hot wire anemometry technique. The radial extent of the vortex core was found to increase with the swirl angle. The measurements are also compared with results for vortex flow in parallel ducts.

NOTATION

f	Frequency	Hz
p'	RMS amplitude of pressure fluctuation	N/m^2
U_2	Rotor tip speed	m/s
Ct	Tangential velocity	m/s
Ca	Axial velocity	m/s
Po	Total pressure	N/m^2
Pa	Ambient pressure	N/m^2
Ψ	Total pressure rise coefficient ($\Delta Po/\rho U_2^2$)	
Φ	Flow coefficient (Q/A_2U_2)	
θ	Vane angle	
β	Nominal inlet swirl angle ($\beta=90^\circ-\theta$)	
R	Radius of fan bellmouth inlet or duct	m

1 INTRODUCTION

Centrifugal fans installed in a system (eg induced draught fans in power stations) are often required to operate at part-load conditions. Inlet vanes are commonly used to adjust the fan operating point because of their low cost compared with a variable speed drive. The vanes impart a pre-whirl in the direction of rotor rotation thus reducing the fan pressure rise and flow rate. However, the swirling flow can cause a central core of dead fluid, the inlet vortex, to form. This core may also precess and take the form of a whirling helical rope, Fig 1.

The inlet vortex can cause strong pressure fluctuations which usually lead to severe noise and vibrations in the fan system. An array of radial vanes (dorsal fins) located on the centreline is commonly used to suppress the inlet vortex. However, no reliable design method exists for dorsal fins. The manufacturer essentially uses cut and try methods and such an approach involves high costs.

Much current knowledge about the inlet vortex in centrifugal fans is based on studies of swirling flows in ducts. Vortex breakdown is said to occur when flow reversal occurs along the axis, ie the original swirling flow with no flow reversal is transformed into one with flow reversal in the central core.

The physics of vortex breakdown in ducts has been studied both experimentally and theoretically (Benjamin, 1962, Squire, 1960, Cassidy and Falvey, 1970, Garg and Leibovich, 1979). Breakdown is known to depend on the ratio of the tangential to axial momentum, ie Ct/Ca, the tangent of the swirl angle. In a theoretical approach (Squire, 1960), the maximum value in the swirl angle distribution along the radius was used as the critical value for the breakdown and the critical swirl angle was found to be 45°-50°. In an experimental study on duct flows (Cassidy and Falvey, 1970), the angular momentum parameter $\Omega D/\rho Q^2$ was used to describe the gross ratio of the tangential to axial momentum, where Ω is the angular momentum flux, Q is the volume flow rate and D is the duct diameter. The critical value of this was found to be about 0.3-0.4 for the breakdown in parallel duct flows at high Reynolds numbers.

The mean axial and tangential velocity distributions measured in a slightly diverging duct using laser doppler anemometry is shown in Fig 2 (Garg and Leibovich, 1979). The axial velocity after breakdown is shown to have a wake-like profile. The tangential velocity increases with radius and reaches the maximum at the core boundary, ie the vortex core behaviour is similar to solid body rotation.

The frequency at which the vortex core precesses and the amplitude of the pressure fluctuations were also experimentally correlated with the gross momentum ratio and were found to be functions of this ratio, ie $fD^3/Q=F(\Omega D/\rho Q^2)$, $p'D^3/\Omega=G(\Omega D/\rho Q^2)$ (Cassidy and Falvey, 1970). For a given duct with a constant momentum ratio the frequency varies linearly with the flow rate. The amplitude of the pressure fluctuations is proportional to the angular momentum flux, ie the square of the flow rate.

In centrifugal fans, the inlet geometry is more complex than a straight duct and thus the results for duct flows may not be transferred directly to the fan. Rotating stall can also occur which can exhibit frequencies similar to the inlet vortex. Rotating stall is a rotating disturbance caused by the interaction of the rotor with the upstream and downstream flow spaces and generally occurs at low flow rates (Chen et al, 1992).

In a study of inlet vortex in centrifugal

fans (Kimura et al, 1986), the vortex frequency found at a high swirl angle (θ=25°) was about twice the frequency found at a low swirl angle (θ=45°) for the same flow coefficient. This was interpreted a vortex of similar rotational speed but with a double cell structure.

In an earlier part of this study (Chen et al, 1992), a dual hot wire technique based on a cross correlation method (Soundra-Nayagam et al, 1990) was used to determine the number of cells in the rotating disturbances and their rotational speed. The inlet vortex condition was then differentiated from the rotating stall condition by carrying out a speed change test. The speed change test makes use of the fact that inlet vortex behaviour is influenced by swirl angle and flow rate and not by rotor speed. In all cases the vortex core was found to have a single cell. The frequency of the velocity fluctuations caused by the inlet vortex was found to have a linear relationship with the flow rate for a given vane angle. This linear relationship was suggested to be used in confirming the existence of an inlet vortex.

In this paper the frequency and amplitude of the pressure fluctuations are presented for the complete range of fan operations and are compared with duct results. Measurements of the variations in the inlet vortex structure are also presented.

2 TEST RIG AND INSTRUMENTATION

The fan is a typical industrial machine and has a geometry representative of larger machines such as those used for power station boiler draught applications. The rotor has 10 backward curved blades, an outlet diameter of 690 mm and an inlet diameter of 440 mm. The outlet and inlet blade angles are 44.1° and 13.9° respectively. The outlet and inlet widths are 62.3 mm and 98.5 mm respectively.

The fan has a bellmouth free inlet with no inlet box and a volute casing discharging into a 610 mm diameter duct. The flow rate was measured using an orifice plate and was controlled by a throttle disc at the duct exit. Inlet vanes were fitted to the fan inlet. The vanes are made of perspex for further flow visualization studies. The vane angle was set in the way that the entering flow had a tangential velocity in the the rotor's moving direction and it could be set between fully closed (θ=0°) and fully open (θ=90°). At fully open the entering flow had no tangential velovity.

Fast response pressure transducers (Druck PDCR 820) were located at different stations along the flow path (inlet bellmouth, rotor exit, casing exit and downstream duct) to measure pressure fluctuations, Fig 3. The length of the plastic tubing connecting each pressure tapping and the transducer sensor was made as short as possible (less than 100 mm) to avoid error due to the resonance in the sensor-tubing system. Transducer signals were passed into two dual-channel digital spectrum analyzers (Advantest TR9402 and Diagnostic Instruments PL22) for spectrum analysis.

A single hot wire probe (DISA P11) was traversed in the throat of the bellmouth (Fig 4). The radial velocity in this section was shown by measurements with a 5-hole probe to be small (less than 10% of the axial velocity). Since the flow structure of the inlet vortex is primarily reflected in the axial velocity distribution, the wire was oriented tangentially to obtain the axial component of velocity. Angular calibration of the hot wire probe indicated that the error was within 10% for a flow angle range of ±60°.

A separate hot wire probe located at a fixed position at the fan inlet was used to provide a trigger signal, Fig 4. The signal from the measuring probe was ensemble averaged over 20 cycles and the averaging was synchronized with the trigger signal (ie phase locked with the vortex). A 200Hz low pass filter was employed to remove high frequency unsteadiness and hence provide a reliable trigger signal. The trigger point was chosen by specifying the level and the slope of the signal (rising or falling). The instrumentation used is also shown in Fig 4.

A 5-hole probe was also used to measure the mean velocity and total pressure distribution in the bellmouth section. The traverse plane was the same as that used for the hot wire measurements.

3 RESULTS AND DISCUSSION

Fan performance tests were carried out over a range of vane angles. A large vane angle corresponds to a low inlet swirl angle with an inlet vane angle of 90° corresponding to the fully open condition. All the results presented here were recorded at a fan speed of 1500 rpm.

Figure 5 shows the non-dimensional fan characteristics and the amplitudes of the pressure fluctuations at different vane angles. The pressure fluctuations shown were recorded using transducer (a_1). An example of the pressure spectrum is shown in Fig 6. The overall amplitude shown includes the contribution of the harmonic peaks.The peak at 50Hz (Fig 6) was due to the instrument noise and was not included in the overall value. A frequency range of 0-200 Hz was used which covered the important frequencies involved. The spectra were averaged over 16 cycles. The amplitude of the pressure fluctuations varied with circumferential position (eg a_1, a_2 and a_3 on the bellmouth) though their spectra showed the same frequency peaks.

The inlet vortex and rotating stall regimes are also shown in Fig 5. The inlet vortex is strong in the middle range of vane angles (θ=60°-37.5°). In this region inlet vortex was detected at all transducer locations with the inlet transducer (a_1) always showing the maximum amplitude, an example for a vane angle of 45° being shown in Fig 8. In the region of θ=30°-15° vane angles, the inlet vortex was only detected at the inlet transducer location, a.

The frequency behaviour is shown in Fig 7. At a constant vane angle, the vortex frequency has a linear relation with the flow rate. The result is in good agreement with the earlier hot wire measurements (Chen et al, 1992). At a constant flow rate, the vortex frequency generally increases with a reduction in the vane angle, ie increased swirl.

The frequency of rotating stall in the fan is independent of vane angle and has an almost constant value of 16 Hz, approximately 2/3 of the rotor passing frequency, Fig 7. In all cases the rotating stall was found to have a single cell. In this paper rotating stall is only indicated at the strong stall conditions (ie fully developed stall cell) though intermittent weak stall conditions may occur prior to the strong stall point (Chen et al 1992). When the vane is fully open (θ=90°) no vortex was found and so a frequency of zero is plotted until rotating stall commences.

The broken lines in Fig 7 represent the regions where the pressure transducers did not give a clear frequency peak due to the weak nature of the inlet vortex or the rotating stall. However, measurements with a hot wire probe located near the inlet of the rotor indicated

that a weak inlet vortex existed towards the high flow coefficient points within the region while a weak intermittent rotating stall existed towards the low flow coefficient points within the region. This suggest that the type and location of sensors affect the sensitivity in detecting flow disturbances.

The frequency variation based on the parallel duct correlation is also shown in Fig 7. The angular momentum parameter, $\Omega D/\rho Q^2$ was calculated from the axial and tangential velocity distributions obtained from the 5-hole probe traverse data where D is the throat diameter of the bellmouth. At a constant vane angle, $\Omega D/\rho Q^2$ was found to be almost constant for different flow coefficients with variation of ±5% and hence the frequency would be expected to vary linearly with the flow rate since $fD^3/Q=F(\Omega D/\rho Q^2)$. The bellmouth and parallel duct results are in good qualitative agreement though there are large differences in the actual frequency values due to the difference between the bellmouth and parallel duct geometry.

Figure 8 shows the amplitude of pressure fluctuation versus flow coefficient taken from different transducer locations at a vane angle of 45°. The transducer in the fan inlet region is seen to be more sensitive than other locations in detecting an inlet vortex. This was also found for vane angles of 60° and 37.5°.

At a constant vane angle, the amplitude of pressure fluctuations (or vortex strength) increased exponentially with the flow coefficient for transducer locations a_1 and b_1. The amplitude of pressure fluctuations versus flow coefficient based on the parallel duct correlation is also shown in Fig 8. This was obtained using the $\Omega D/\rho Q^2$ value calculated from the 5-hole probe data.

Hot wire traversing was carried out for different vane angles and flow rates. Axial velocity contours were then obtained from the hot wire traverse data. Figure 9 shows examples obtained for three different vane angles at the same flow coefficient. The hatched area may be taken to represent the vortex core. A single cell structure is plotted, based the cross correlation findings. It is seen that the vortex core has an asymmetric shape.

Distributions of mean velocity and total pressure along the radius were obtained from the 5-hole probe traverse data. Figure 10 shows the results for different flow coefficients at a constant vane angle of 45°. Figure 11 shows the results for different vane angles at a constant flow coefficient.

A comparison has been made between the experimental results and the predictions of a theoretical model (Eck, 1973). The model is for a parallel duct flow with a free vortex tangential velocity distribution before vortex breakdown. The comparison with the model was made using the ratio of the tangential velocity to axial velocity. For the experimental data the tangential velocity was calculated from the mass weighted angular momentum. Theoretical vortex core radii, $(r_c/R)_{th}$, have been plotted in Figs 10 and 11.

At a constant vane angle (Fig 10), as the flow coefficient increases both the axial and tangential velocity components before entering the vortex core increase to keep the momentum ratio constant. The fluid is slowed down as it enters the core and this process involves losses. Therefore, the total pressure drop also increases with flow coefficient as seen in Fig 10.

At a constant flow coefficient (Fig 11), as the swirl angle increases the tangential velocity increases so that the velocity before entering the core increases. Thus the total pressure drop will also increase with the swirl angle.

Since the vortex core radius is constant for a given vane angle, It may be expected that dorsal fins would be equally effective at all flow rates. However, the change in vortex core radius with vane angle means that dorsal fins designed to control the inlet vortex at some vane angles may not do so at other vane angles. Large dorsal fins would be expected to have a greater vortex control effect but would increase the power penalty. A variety of vortex control devices are now being studied at NEL.

4 CONCLUSIONS

The inlet vortex behaviour in the bellmouth inlet of a centrifugal fan is similar to that of vortex flow in a duct. It is not influenced by the fan rotor. The vortex frequency was found to increase linearly with flow rate for a constant swirl angle. For a constant flow rate the frequency also increased with swirl angle. The core of the inlet vortex was asymmetric and had a single cell structure. The radius of the core increased with swirl angle. However, it did not change with the flow rate for a constant swirl angle.

The strongest pressure fluctuations caused by the inlet vortex occurred in the middle range of vane angles. For a constant vane angle the amplitude of pressure fluctuations increased exponentially with flow rate. The maximum fluctuation occurred at the fan inlet with a rapid decay in amplitude for stations further downstream.

ACKNOWLEDGMENTS

The present work is part of a collaborative research programme with the University of Strathclyde. The Ph.D study programme of the first author is supported by the British Council and Chinese Government. This paper is published with the permission of the Chief Executive, National Engineering Laboratory and is Crown copyright.

REFERENCES

BENJAMIN, T B (1962) Theory of the vortex breakdown phenomenon. J Fluid Mech, v14, 593-629

CASSIDY, J J and FALVEY, H T (1970) Observations of unsteady flow arising after vortex breakdown. J Fluid Mech, v41, 727-736.

CHEN, P, SOUNDRA-NAYAGAM, M, BOLTON, A N and SIMPSON, H C (1992) Unstable flows in centrifugal fans. Proc IMechE Conf on Power Station Pumps and Fans, London, 25-32.

ECK, B (1973) Fans, Pergamon Press, 265-267

GARG, A K and LEIBOVICH, S (1979) Spectral characteristics of vortex breakdown flow fields. Phys Fluids, v22, n11, 2053-2064.

KIMURA, Y, HIGASHIMORI, H and WATABIKI, N (1986) Characteristics of pressure pulsations and mechanisms of an inlet cone vortex in centrifugal fans. Nippon Kikai Gakkai Ronbunshu B Hen, v52, n480, 2939-2946.

SOUNDRA-NAYAGAM, M, BOLTON, A N and MARGETTS, E J (1990) Dynamic flow measurements on model fan. National Engineering Laboratory, Report No 272/90.

SQUIRE, H B (1960) Analysis of the vortex breakdown phenomenon. Report No 102, Department of Aerospace Engineering, Imperial College, London.

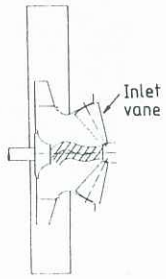

Fig 1 Inlet vortex

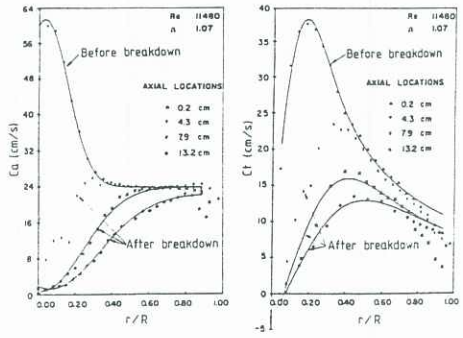

Fig 2 Velocity profiles after vortex breakdown in a duct (Garg and Leibovich, 1979)

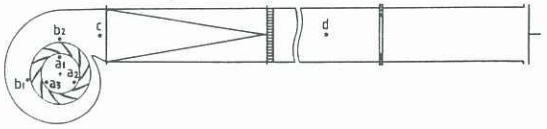

Fig 3 Pressure transducer locations

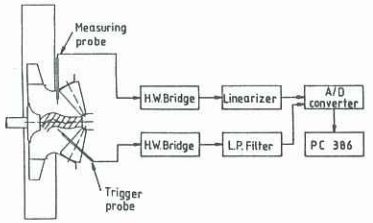

Fig 4 Hot wire traverse instrumentation

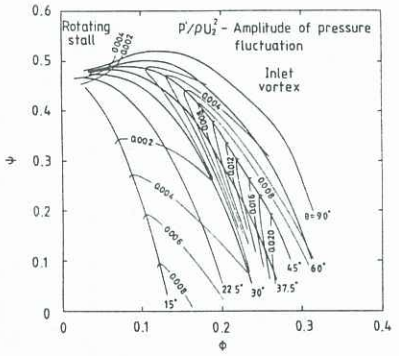

Fig 5 Amplitude of pressure fluctuations (a_1)

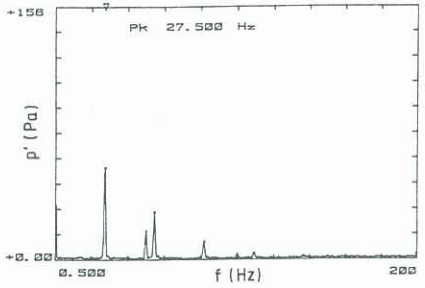

Fig 6 Inlet vortex pressure spectrum (a_1)

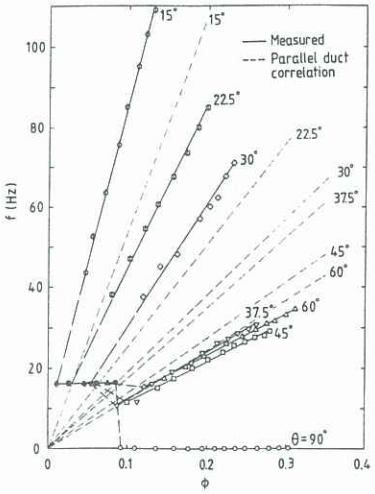

Fig 7 Inlet vortex frequency behaviour (solid symbols - strong stall points)

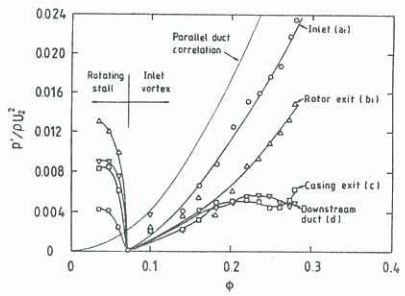

Fig 8 Amplitude of pressure fluctuations at different transducer locations (θ=45)

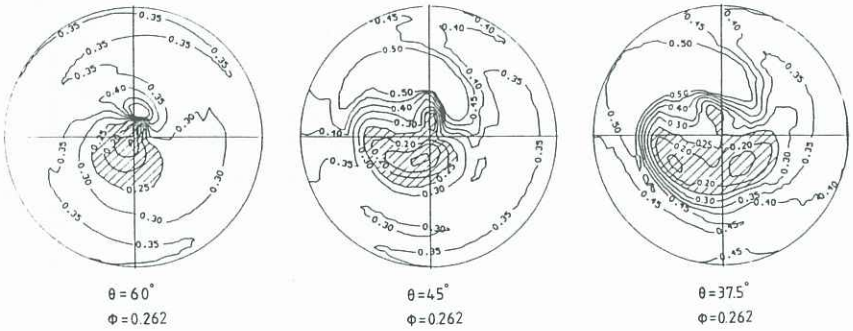

Fig 9 Variation of the inlet vortex axial velocity contours

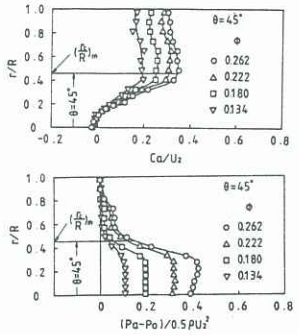

Fig 10 Variation of mean flow with flow coefficient

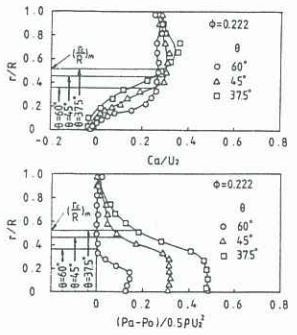

Fig 11 Variation of mean flow with vane angle